Tantalum Carbide and Nitride Diffusion Barriers for Cu Metallisation

T. Laurila[a)] , K. Zeng and J.K. Kivilahti
Lab. of Electronics Production Technology,P.O.Box 3000, FIN-02015 HUT, Finland

J. Molarius, T. Riekkinen and I.Suni
VTT Microelectronics, P.O.Box 1101, FIN-02044 VTT, Finland

ABSTRACT

The reactions in the Si/TaC/Cu and Si/Ta_2N/Cu metallisation systems were investigated by x-ray diffraction, Rutherford backscattering, scanning electron microscope and the transmission electron microscopy. The results were then combined with the assessed ternary Si-Ta-C, Ta-C-Cu, Si-Ta-N and Ta-N-Cu phase diagrams. It was found that both barriers ultimately failed due to diffusion of Cu through the barrier and accompanied formation of Cu_3Si at temperatures higher than 725 °C. However, in the TaC barriers the formation of amorphous TaO_x layer with significant amounts of C took place at the TaC/Cu interface already at 600 °C. Similar behaviour at "low" temperatures was also noted in the Ta_2N barriers.

Keywords: Phase diagrams; diffusion barriers; copper metallisation, tantalum carbide; tantalum nitride

a) corresponding author, e-mail: Tomi.Laurila@hut.fi

1. INTRODUCTION

Interest in copper for conduction lines and structures has been wide, since it offers many advantages over the currently used Al based materials. Unfortunately, the interaction between Si and Cu is strong and detrimental to the electrical performance of Si even at temperatures below 200 °C[1-3]. Thus, it is necessary to implement a barrier layer between Si and Cu. Refractory metals such as tantalum are frequently suggested to be used as barrier layers in Cu metallised IC's. However, according to our investigations thin elemental Ta barrier layers may not posses sufficient stability when in contact with Si and Cu[4]. In order to improve the performance of the barrier layers it is essential to understand the underlying mechanisms leading to the failure. This can be achieved by using a combined thermodynamic and kinetic approach. By utilising this method it was found that the use of binary tantalum compounds like tantalum nitride and tantalum carbide could improve the performance of the barrier layers. The phase relations in the Si/TaC/Cu and Si/Ta_2N/Cu metallisation systems are examined with the help of the calculated ternary phase diagrams. The information extracted from these diagrams are coupled with the experimental results obtained to reveal the mechanism(s) leading to the failure.

2. MATERIALS AND METHODS

The Cu, TaC and Ta_2N films were sputtered onto cleaned and oxide-stripped (100) oriented n-type Si substrates in a cluster sputtering tool. The base pressure before the deposition was about 3×10^{-5} Pa. Both diffusion barriers were rf-magnetron sputtered, Ta_2N in argon/nitrogen gas-mixture from the elemental target whereas TaC was obtained from the

compound target in argon atmosphere. Barrier thicknesses were about 10, 50 and 100 nm for Ta_2N and 7, 35, and 70 nm for TaC, as determined with RBS. The copper films (100 or 400 nm) were subsequently sputtered onto Ta_2N and TaC films from the dc-magnetron target without breaking the vacuum. The samples were then annealed in the vacuum of about 10^{-4} Pa at temperatures from 500 to 800 °C for 30 min. The reactions in the metallisation schemes were investigated by the sheet resistance measurements, grazing incidence x-ray diffraction (XRD), Rutherford backscattering spectroscopy (RBS), scanning electron microscope (SEM) and the transmission electron microscopy (TEM). The results of the experimental investigations were compared with the assessed phase diagrams. Ternary Si-Ta-C, Ta-C-Cu, Si-Ta-N and Ta-N-Cu phase diagrams were calculated from the assessed binary thermodynamic data [5-10] and compared with the experimental results obtained.

3. RESULTS AND DISCUSSION

The sheet resistance measurements vs. temperature of the Si/TaC(70nm)/Cu(400nm) samples showed an abrupt rise in the sheet resistance at 775 °C indicating that a reaction had occurred. The 7 nm and 35 nm TaC layers were stable up to 550 °C and 650 °C, respectively. The rise in the sheet resistance was accompanied with the loss of shiny copper-like appearance of the sample surface, regardless of the thickness. The SEM micrograph of the surface of the 70 nm TaC sample annealed at 800 °C is shown in Fig. 1(a). Large "squares" have formed on the surface (about 20-30 μm in diameter). These "squares" are surrounded by a "flowery" patterned structure, which seems to consist of one phase embedded into another.

The sheet resistance measurements of the Si/Ta_2N(100nm)/Cu(400nm) showed an abrupt rise in the sheet resistance at 775 °C and the samples with 10 and 50 nm Ta_2N layers were stable up to 625 °C and 675 °C, respectively. The surfaces of the Ta_2N samples maintained their shiny copper-like appearence up to 750 °C (100 nm), 650 °C (50 nm) and 600 °C (10 nm). The structure formed on the surface after reaction(s) was very similar to that observed in the TaC films. The SEM micrograph of the surface structure of the sample with 100 nm Ta_2N barrier annealed at 775 °C is shown in Fig. 1(b).

The RBS analyses of the as deposited TaC samples showed sharp edges of the elements in the spectra indicating that the layers were clearly discrete at this stage. The spectra from the annealed samples with the 70 nm thick TaC layers showed that some reaction(s) had taken place already at 600 °C (Fig.2). As can be seen, the spectrum has been graded and tantalum has moved towards the surface. This indicates that the TaC layer has decomposed, which is not expected based on the high thermal stability of TaC compound. From the spectra taken at higher temperatures, it was very difficult to obtain more information about the reactions taking place, as the surface of the samples did not stay planar (see Figs. 1 (a) and (b)) the interpretation of RBS spectrum was not unambigious.

The RBS analyses of the as deposited Ta_2N samples showed also clearly discrete layers before the annealings. The layer thicknessess were about 10, 50 and 100 nm. The spectra from the sample with 100 nm thick Ta_2N layers showed that some reaction(s) took place at 650 °C (Fig. 3). The temperature was again unexpectedly low as with the TaC layers. At higher temperatures the spectra further degraded and no additional information could be obtained.

Hence, the RBS results showed that something unforeseen took place at low temperatures in both metallisation systems.

In order to obtain information about the phase formation during the annealings the XRD analyses were conducted. The results (Fig. 4) from the Si/TaC(70nm)/Cu(400nm) samples showed that up to 725 °C there were only TaC and Cu present in the 70 nm TaC samples. At 725 °C there were some weak diffractions also from Ta_2O_5, showing the presence of oxygen in the annealing ambient and in the metallisation structure. At 750 °C the formation of Cu-silicide (Cu_3Si) took place. However, the analyses showed that Cu_3Si was not present as its usually cited structure and the peaks were not "stable". At 800 °C, the TaC and Cu peaks had disappeared and only Cu_3Si and $TaSi_2$ peaks were present. According to the phase diagram (Fig. 7(b)) and the mass balance requirement, the formation of SiC should also have taken place. However, it was not detected in the XRD analysis. Moreover, no indication of reaction(s) at 600 °C was detected contrary to the RBS results. TaC diffusion barriers showed better performance with increasing thickness. Failure temperature increased from 600 (7nm) to 675 (35nm) to 750 ^{o}C (70nm). Despite the different thickness of the films the failure seemed to be induced by Cu penetration through the TaC layer and the formation of Cu_3Si.

X-ray diffractograms (Fig. 5) of the annealed Si/Ta_2N(100nm)/Cu(400nm) structures showed unexpected peaks after annealing at 700 ^{o}C. Peak positions suggested a hexagonal phase, which was designated as Ta_xN phase[12], because we were unable to identify it from standard x-ray patterns. However, the peaks also fitted quite well to a Ta_xO type phase and therefore may be used as an indication from the presence of oxygen in the annealing ambient as well as in the

metallisation structure itself. However, this must be further verified. The 100 nm Ta_2N diffusion barriers failed by the formation of Cu_3Si phase at 775 °C. Failure temperature increased from 650 to 725 to 775 ^oC as film thickness increased from 10 to 50 to 100 nm in the same way as in TaC barriers. No reactions between Ta_2N and the Si substrate were detected contrary to the observations in the TaC system, where $TaSi_2$ formed at higher temperatures. Presently it seems that performance of the Ta_2N as well as TaC barriers is mainly dominated by "defects" in the films. These "defects", e.g. grain boundaries, offer fast diffusion paths for copper atoms, which will then react with silicon by forming copper silicide, Cu_3Si. However, in both systems something unexpected takes place at relatively low temperatures as showed by RBS.

In order to clarify the puzzling RBS results at 600 °C, the cross-sectional TEM specimen was prepared from the 70nm TaC sample. The micrograph presented in Fig. 6 shows the presence of an amorphous layer between TaC and Cu. The amorphous nature of the layer was further verified with HREM investigations and electron diffraction patterns.[11] The layer consisted mainly of Ta with significant amounts of C and O as showed by x-ray energy dispersive spectrometry (XEDS) analyses (expected to be metastable TaO_x layer with C released in the decomposition of the TaC layer). As can be seen from Fig. 6, the TaC layer consists of large elongated columnar grains. This should offer suitable short-circuit paths for Cu diffusion. The fact that significant Cu diffusion was not detected was attributed to the oxygen rich amorphous layer present at the TaC/Cu interface, which formed an additional diffusion barrier to Cu diffusion. The formation of the layer was induced by diffusion of oxygen to the interface from the annealing environment and also from the films themselves. The stability of TaO_x is expected to be so high that it was able to decompose the TaC layer and the formation of the

observed amorphous interlayer took place. However, this must be verified with detailed thermodynamic description of the Ta-C-O system, which is currently under construction. The carbon found in the amorphous layer is a result of the dissociation of TaC layer at the TaC/Cu interface. Only after suitable high temperature is reached, the amorphous layer is partly or completely crystallised and the diffusion of Cu will proceed. The observation of the amorphous interlayer formation between TaC and Cu gives some indication why the RBS spectrum has degraded already at 600 °C. From the sample annealed at 750 °C (Fig. 7) one could observe Si-O, TaO_x along with the very large Cu_3Si protrusions. This shows that at 750 °C Cu atoms have been able to diffuse through the partly crystallised amorphous layer to the Si/TaC interface and the formation of Cu_3Si has taken place. However, no crystalline tantalum silicides were detected and there was still large amount of the amorphous oxide rich layer present. At still higher temperatures (800 °C) XTEM investigations showed the formation of $TaSi_2$ and SiC, which was expected based on the thermodynamic evaluation of the metallisation system. Similar behaviour is also anticipated to take place in the Ta_2N films at 650 °C, since it seems that the annealing ambient as well as the films contained some oxygen also in Ta_2N case (see the XRD results) and the RBS results showed similar behaviour in comparision to the TaC films. Unfortunately detailed TEM results are not yet available.

The phase relationships in the Si-Ta-C, Si-Ta-N, and in the Ta-C-Cu, Ta-N-Cu phase diagrams are very similar. Figure 8 (a) shows the evaluated isothermal section of the ternary Ta-C-Cu phase diagram. It can be seen that Cu is in equilibrium with both TaC and Ta_2C. Thus, the reactions at the interface Cu/TaC do not have driving force because the interface is already in local thermodynamic equilibrium. Nevertheless, the driving force for copper diffusion through

barrier towards silicon is expected to be substantial, since copper has a very high affinity towards silicon. Figure 8 (b) shows the isothermal section of the calculated Ta-Si-C ternary phase diagram. There are two important issues, which have to be carefully considered in the calculations due to the lack of reliable experimental information. However, they have been discussed previously elsewhere [13] and are not repeated here. It can be seen that at the Si/TaC interface there exist a driving force for reaction between the substrate and the TaC layer, since there is no TaC-Si equilibrium in the ternary phase diagram(Fig. 8(b)). In fact, reactivity of this interface was manifested by the experimentally observed formation of $TaSi_2$ and SiC at 800 °C. Figure 9 (a) shows the isothermal section from the Ta-N-Cu diagram. The same thermodynamic considerations about the barrier/Cu interface, as in the carbide case, are also valid here. Figure 9 (b) shows the isothermal section from the Si-Ta-N phase diagram. Again the similarity is evident. Hence, the systems resemble each other very closely. As expected on the basis of the thermodynamic properties of the metallisation systems, the failure mechanisms were found to be of similar kind. No reactions between Si and Ta_2N were detected in this investigation up to 775 °C and the failure occurred by the formation of Cu_3Si, thus indicating considerably stability of the Si/Ta_2N interface.

CONCLUSIONS

The interfacial reactions in the Si/TaC/Cu and Si/Ta_2N/Cu systems were investigated. The diffusion of Cu through the barrier and the accompanied formation of Cu_3Si ultimately caused the failure of both of the barrier layers. The stabilities of the TaC and Ta_2N layers were found to be reasonably high and of similar magnitude. However, both systems exhibited similar kind of intriguing reaction at low temperatures (600 °C for TaC and 650 °C for Ta_2N). In the

TaC case the reaction was found to be an amorphous TaO_x layer formation at the TaC/Cu interface. Formation of similar kind of layer is also expected to take place in the Si/Ta_2N/Cu system. The observed similarities in the behaviour of the carbide and nitride films can be understood with the help of the corresponding evaluated Si-Ta-C, Si-Ta-N, Ta-C-Cu and Ta-N-Cu ternary phase diagrams, which show almost identical phase relationships.

ACKNOWLEDGEMENTS

Authors greatly acknowledge J. Saarilahti and A. Nurmela from the VTT Microelectronics for help in the RBS analyses. The work was financially supported by the Academy of Finland.

References:

[1] A.A. Istratov and E.R. Weber, Electrical Properties and Recombination Activity of Copper, Nickel and Cobolt in Silicon, Appl. Phys. A, **66**, (1998) 123-136.

[2] S.P. Murarka, Advanced Materials for Future Interconnections of the Future Need and Strategy, Microelectronic Engineering, **37/38**, (1997) 29-37.

[3] C-A. Chang, Formation of Copper Silicides from Cu(100)/Si(100) and Cu(111)/Si(111) Structures, J. Appl. Phys. **67**, (1990), 566-569.

[4] T.Laurila, K. Zeng, J.K. Kivilahti, J. Molarius and I. Suni, Failure Mechanism of Ta Diffusion Barrier Between Cu and Si, J. Appl. Phys., **88**, (2000) 3377-3384.

[5] J. Lacaze and B. Sundman, An Assessment of the Fe-C-Si System, Metall. Trans. A, **22**, (1991), 2211-2223.

[6] K. Frisk and A. F. Guillermet, Gibbs Energy Coupling of the Phase Diagram and Thermochemistry in the Tantalum-Carbon System, J. Alloys Compd., **238**, (1996),167-178.

[7] L. Chandra Sekaran, Cu-Fe-P-C, Report , Data in Thermo-Calc, (1987).

[8] K. Frisk, A Thermodynamic Evaluation of the Fe-Cu-C-N System, Report IM-2929, Swedish Institute for Metals Research, Stockholm.

[9] M. Hillert, S. Jonsson, and B. Sundman, Thermodynamic Calculation of the Si-N-O System, Z. Metallkde., **83**, (1992), 648-654.

[10] K. Frisk, Analysis of the Phase Diagram and Thermochemistry in the Ta-N and the Ta-C-N Systems, J. Alloys Compd., **278**, (1998), 216-226.

[11] T.Laurila, K. Zeng, J.K. Kivilahti, J. Molarius and I. Suni, TaC as a Diffusion Barrier Between Cu and Si, to be submitted.

[12] J. Molarius, T. Riekkinen, I. Suni, T. Laurila, K.Zeng and J.K. Kivilahti, Reactively Sputtered Ta_2N and TaN Diffusion Barriers for Copper Metallization, Advanced Metallization Conference 2000 (AMC), San Diego, CA, 3-5 Oct., (2000), 137-138.

[13] T.Laurila, K. Zeng, J.K. Kivilahti, J. Molarius and I. Suni, Reliability of Tantalum Based Diffusion Barriers between Copper and Silicon, 2000 MRS Spring Meeting (Materials Research Society), San Francisco CA, 24-28 April, **v612**, (2000), 97.

FIGURE CAPTIONS

FIG.1. (a) SEM micrograph from the surface of the Si/TaC(70nm)/Cu(400nm) sample annealed at 800 °C for 30 min and (b) SEM micrograph from the surface of the Si/Ta_2N(100nm)/ Cu(400nm) sample annealed at 775 °C for 30 min.

FIG.2. RBS spectra (2.0 MeV 4 He^+, θ = 170 °) from the Si/TaC(70nm)/Cu(400nm) samples annealed at different temperatures for 30 min. Vertical arrows represent surface scattering energies.

FIG.3. RBS spectra (2.0 MeV 4 He^+, θ = 170 °) from the Si/Ta_2N(100nm)/Cu(400nm) samples annealed at different temperatures for 30 min. Vertical arrows represent surface scattering energies.

FIG.4. XRD spectra from the Si/TaC(70nm)/Cu(400nm) samples annealed at different temperatures.

FIG. 5. XRD spectra from the Si/Ta_2N(100nm)/Cu(400nm) samples annealed at different temperatures.

FIG.6. Bright field cross-sectional TEM micrograph from the Si/TaC(70nm)/Cu(400nm) sample annealed at 600 °C for 30 min.

FIG.7. Bright field cross-sectional TEM micrograph from the Si/TaC(70nm)/Cu(400nm) sample annealed at 750 °C for 30 min. Original surface is on the top of the figure.

FIG.8. (a) Isothermal section at 700 °C from the ternary Ta-C-Cu phase diagram (b) isothermal section at 700 °C from the ternary Si-Ta-C phase diagram.

FIG.9. (a) Isothermal section at 700 °C from the ternary Ta-N-Cu phase diagram, (b) isothermal section at 700 °C from the ternary Si-Ta-N phase diagram.

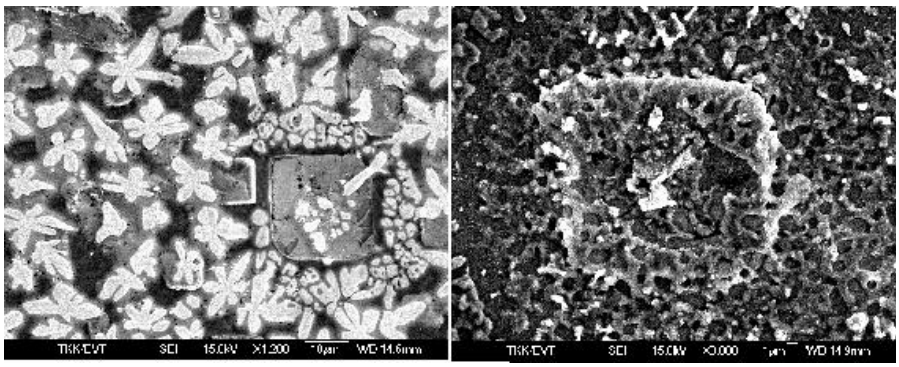

(a) **(b)**

Fig. 1

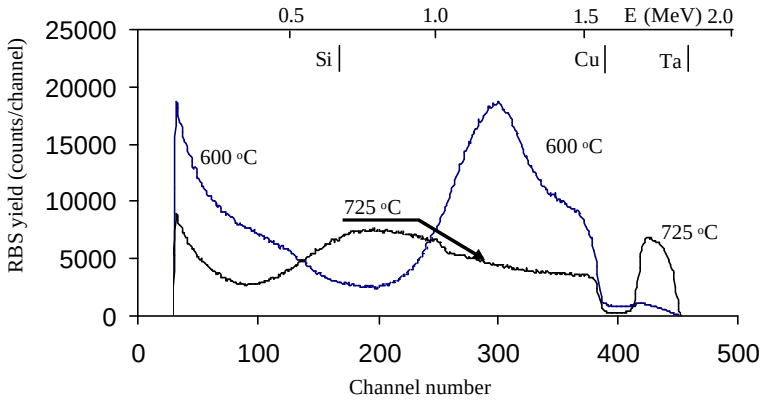
0.5
1.0
1.5
E (MeV) 2.0
Si
Cu
Ta
25000
20000
15000
10000
5000
0
RBS yield (counts/channel)
600 °C
725 °C
600 °C
725 °C
0
100
200
300
400
500
Channel number

Fig. 2

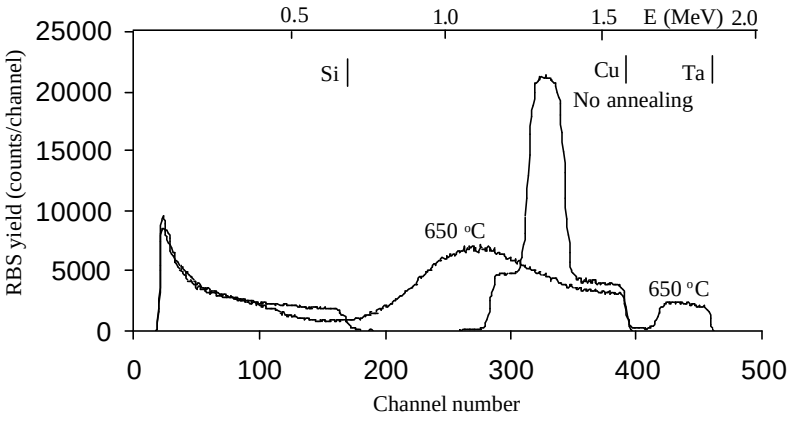
0.5
1.0
1.5
E (MeV)
2.0
25000
20000
15000
10000
5000
0
RBS yield (counts/channel)
Si
Cu
Ta
No annealing
650 °C
650 °C
0
100
200
300
400
500
Channel number

Fig. 3

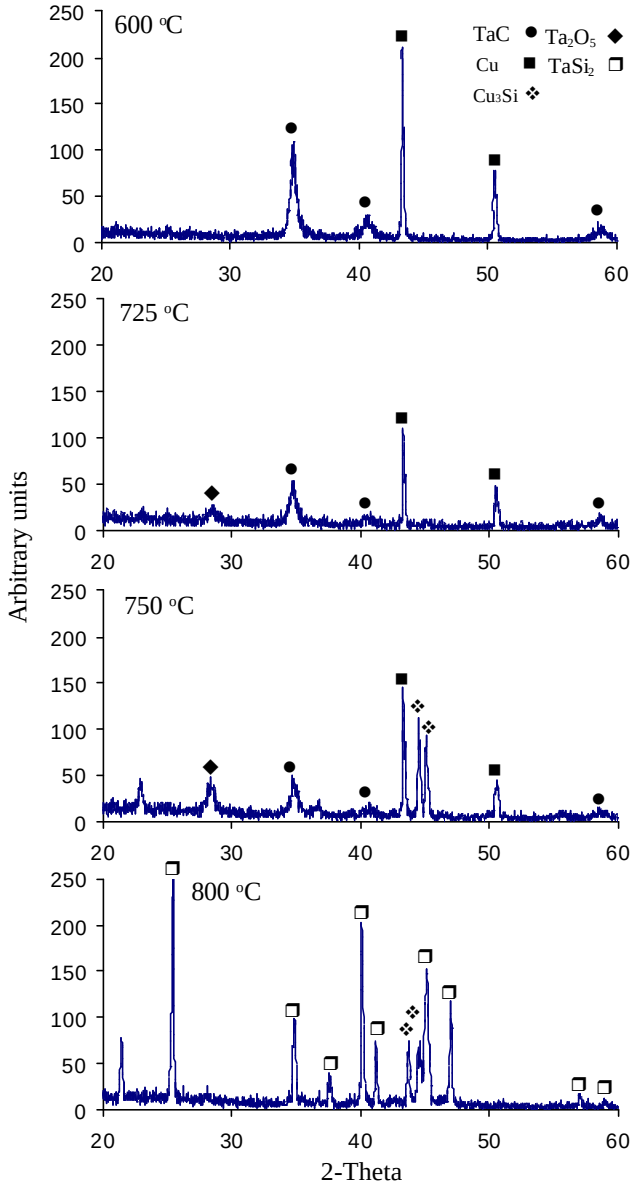
600 °C
725 °C
750 °C
800 °C
TaC ● Ta2O5 ◆
Cu ■ TaSi2 ❒
Cu3Si ❖
Arbitrary units
2-Theta
0
50
100
150
200
250
20
30
40
50
60

Fig. 4

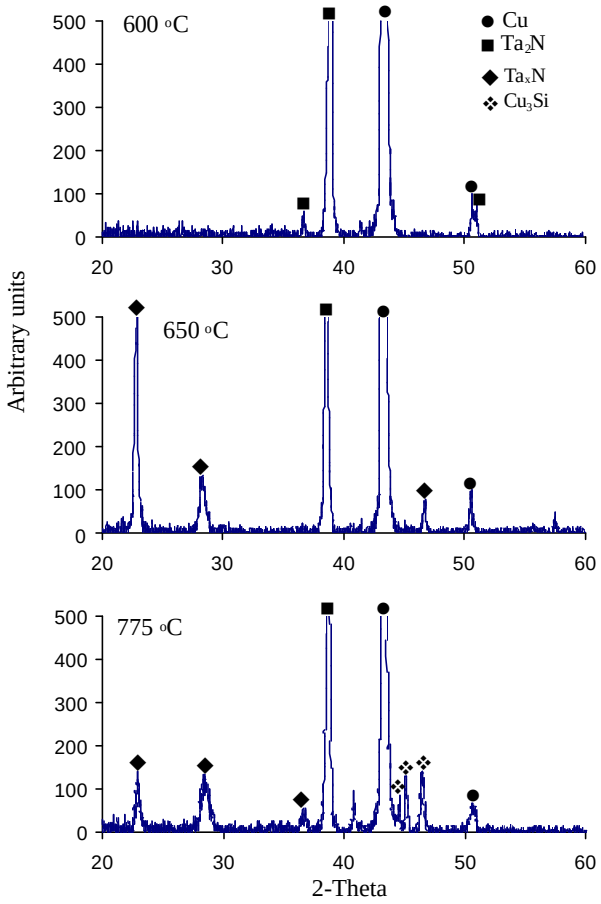
600 °C
650 °C
775 °C
● Cu
■ Ta2N
◆ TaxN
❖ Cu3Si
Arbitrary units
2-Theta
0
100
200
300
400
500
20
30
40
50
60

Fig. 5

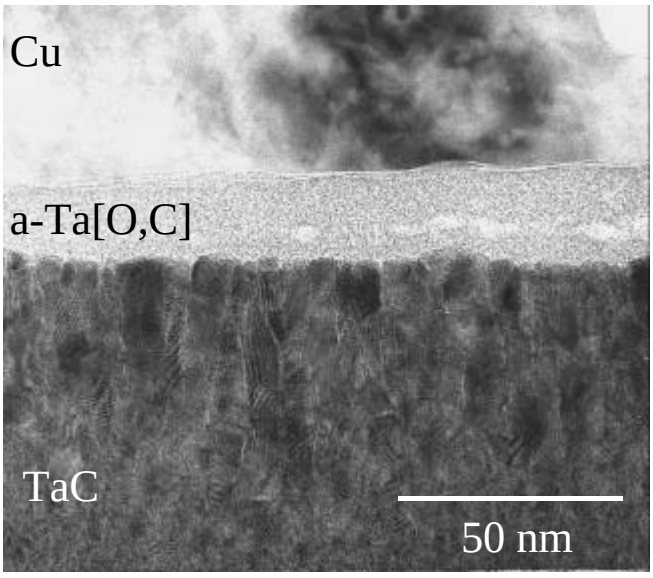

Fig. 6

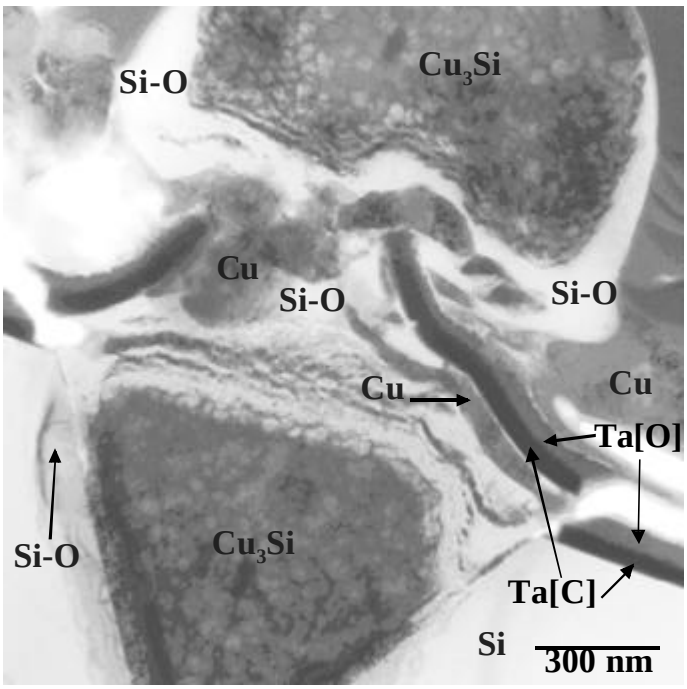

Fig. 7

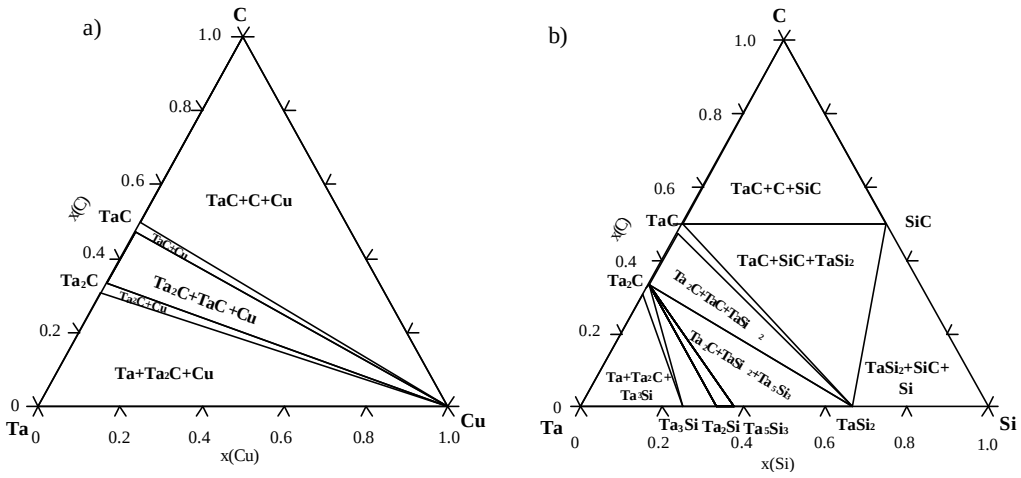
a)
C
1.0
0.8
0.6
0.4
0.2
0
x(C)
TaC
Ta2C
TaC+C+Cu
TaC+Cu
Ta2C+TaC+Cu
Ta2C+Cu
Ta+Ta2C+Cu
Ta
Cu
0
0.2
0.4
0.6
0.8
1.0
x(Cu)
b)
C
TaC+C+SiC
TaC
SiC
TaC+SiC+TaSi2
Ta2C
Ta2C+TaC+TaSi2
Ta2C+TaSi2+Ta5Si3
Ta+Ta2C+
Ta5Si
TaSi2+SiC+
Si
Ta3Si
Ta2Si
Ta5Si3
TaSi2
Si
x(Si)

Fig. 8

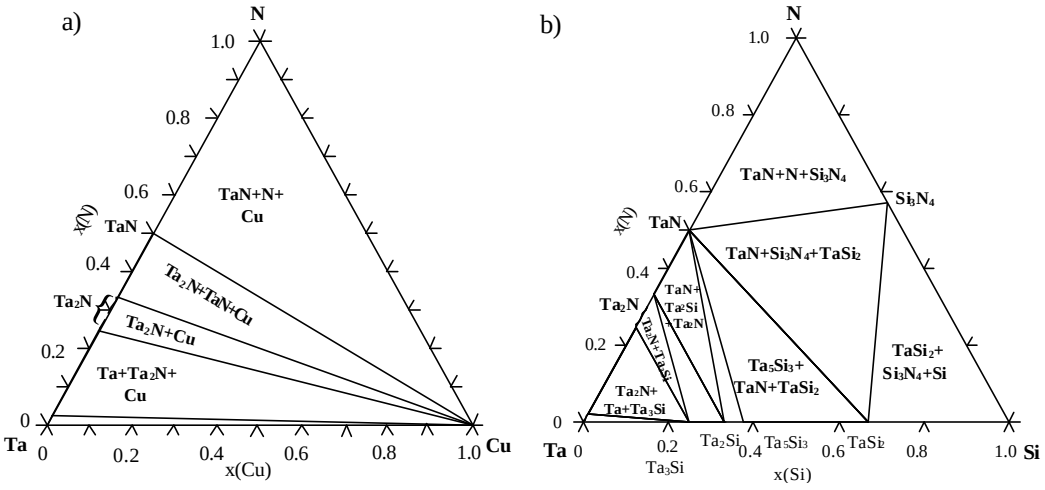
a)
N
1.0
0.8
0.6
0.4
0.2
0
x(N)
TaN
Ta2N
C
TaN+N+
Cu
Ta2N+TaN+Cu
Ta2N+Cu
Ta+Ta2N+
Cu
Ta
Cu
0
0.2
0.4
0.6
0.8
1.0
x(Cu)
b)
N
TaN+N+Si3N4
Si3N4
TaN
TaN+Si3N4+TaSi2
Ta2N
TaN+
Ta2Si
+Ta2N
Ta2N+Ta5Si3
Ta5Si3+
TaN+TaSi2
TaSi2+
Si3N4+Si
Ta2N+
Ta+Ta3Si
Ta
Si
Ta3Si
Ta2Si
Ta5Si3
TaSi2
x(Si)

Fig. 9